PERFORMANCE EVALUATION OF THE TRAVELING WAVE-BASED DIFFERENTIAL PROTECTION WHEN APPLIED ON HYBRID TRANSMISSION LINES

F. V. Lopes*, C. M. S. Ribeiro*, J. P. G. Ribeiro*, E. J. S. Leite Jr.*

*Department of Electrical Engineering, University of Brasília, Brazil,
felipevlopes@unb.br, cmsr@aluno.unb.br, joaopauloribeiro@aluno.unb.br, eduardoleite@aluno.unb.br

Keywords: Hybrid lines, differential protection, time-domain line protection, traveling waves, TW87.

Abstract

This paper evaluates the traveling wave-based differential protection (TW87) when applied on hybrid transmission lines (HTL). The TW87 has attracted the interest of utilities due to its high-speed operation and reliability. However, to apply such a function on lines that combine overhead and underground cable sections, additional challenges arise, which must be overcome to guarantee the proper TW87 operation. The goal of this paper is to clarify issues related to the TW87 settings and performance when applied on HTLs, highlighting the impact of the used settings on the protection operation. To do so, fault scenarios on a 230 kV/60 Hz test power system were simulated using the Alternative Transients Program (ATP). The obtained results attest the TW87 is able to properly protect HTLs, provided that special requirements are considered.

1 Introduction

In recent decades, electrical power systems have grown rapidly. As a result, transmission lines have been requested to operate close to their stability limits, what has been cause of concern for utilities [1]. To overcome transient stability problems, researchers and relay manufacturers have made efforts to develop high-speed protection functions with the aim to speed up the fault clearance procedure, increasing the stability margins of power grids [2].

Among the existing high-speed protection functions, the traveling wave-based differential line protection, called TW87, has shown to be reliable and fast, achieving tripping times in the order of a few milliseconds [3]. The TW87 evaluates the first incident fault-induced traveling waves (TWs) that reach both line terminals and those ones that show up at the line ends one line propagation time after the first detection [2]. By doing so, when applied in parallel with a companion phasor-based relay, in less adverse scenarios, the well-known reliability of the traditional protection functions is maintained, whereas the protection operation is accelerated in critical fault cases, which are those that deserve more attention regarding transient stability issues [3], [4].

In the context of modern transmission networks, HTLs have been more and more used. HTLs combine overhead transmission lines (OTL), underground cable lines (UCL) and not so rare underwater cables [5]. Depending on the differences between the electrical parameters of each section, TWs may propagate with different velocities, affecting TW-based protection and fault location functions which consider an uniform propagation velocity along the monitored line [6].

According to the TW87 developers, due to the different parameters on HTLs, some adaptations and system topology conditions must be taken into account to guarantee a reliable TW87 operation [7]. However, in the open literature, a detailed analysis justifying these adaptations and conditions has not been found. Hence, in this paper, the performance of the TW87 when applied on HTLs is evaluated. Different protection settings are studied and different fault scenarios are simulated using the ATP, allowing the analysis of key issues related to the TW87 application on HTLs. The obtained results show that the TW87 properly operates when applied on HTLs, provided that the specific requirements and settings suggested reported by the TW87 developers are considered.

2 The TW87 Function

The main operation conditions of the TW87 function are based on the analysis of current TW that enter and leave the monitored transmission line [2], [4]. To better illustrate the main principles of the TW87, Figure 1 depicts the Lattice diagrams for internal and external faults on an overhead line.

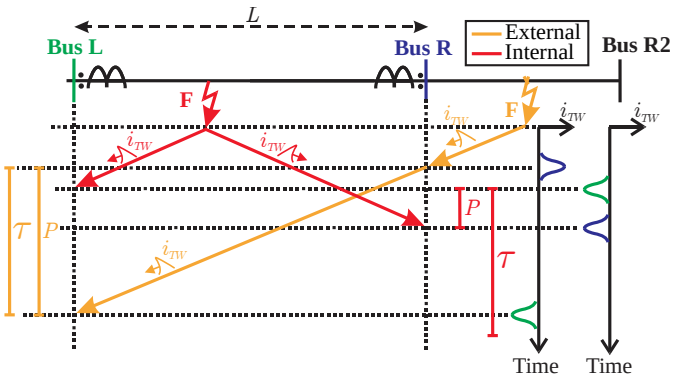

Figure 1: Lattice diagrams for internal and external faults.

From Figure 1, according to the polarity of local and remote current transformers (CTs), it is noticed that TWs that enter and leave the line have opposite polarities. Also, it should be observed that the time lag P between the instants at which the first TWs reach the monitored terminals is approximately the line propagation time τ in external fault cases, (i.e., $P \approx \tau$), and smaller than τ for internal faults (i.e., $P < \tau$). Based on these assumptions, the TW87 computes operating and restraining current signals, which are obtained using:

$$i_{OP}(t) = i_{TWL}(t-P) + i_{TWR}(t)], \quad (1)$$

$$i_{RT} = \max[\, i_{RTL}, i_{RTR}\,], \quad (2)$$

being:

$$i_{RTL}(t) = \left| i_{TWL}(t-\tau) - i_{TWR}(t) \right|, \quad (3)$$

$$i_{RTR}(t) = \left| i_{TWR}(t-\tau) - i_{TWL}(t) \right|, \quad (4)$$

where i_{TWL} and i_{TWR} are the amplitudes of the first TWs that reach the local and remote line terminals, respectively.

By analyzing (1) to (4), and considering the abovementioned relations between P and τ, as well as the local and remote terminal TW polarities, in internal fault cases, i_{OP} increases, whereas i_{RT} tends to have small values. On the other hand, for external faults, i_{OP} tends to present small values, whereas i_{RT} increases. From these conditions, the TW87 distinguishes internal from external faults on transmission lines.

Regarding the TW87 numerical implementation, the following aspects must be considered:

1) The first step of the TW87 is the extraction of TWs from the monitored current signals. Such a procedure is performed by means of the differentiator-smoother filter (DS filter) [8], which has shown to be suitable for TW-based applications. As TWs induce step-changes in the monitored signals, the DS filter was developed to respond to step-changes with a triangular-shaped output, whose peak value is associated to the TW arrival time at the monitored terminal. Even in cases of attenuated transients in which ramp-changes would show up instead of step-changes, the DS filter would respond with a parabola-shaped output, whose peak can be also associated with the TW arrival time [8]. As reported in [7], the DS filter has a window length of 20 µs, and the peak value of the triangular-shaped outputs occur at half the DS filter length, i.e., 10 µs after the moment at which the DS filter window enters in the signal transient period. In the TW87, the samples at which the first incident TWs are detected at the local e remote terminals are called NL_{FIRST} and NR_{FIRST}, respectively. To facilitate the next explanations, the DS filter window length will be referred to as T_{DS};

2) Once the first incident TWs are detected, search windows with length equal to T_{DS} (the same length of the DS filter) are created to identify wavefronts that leave the line in external fault cases. Basically, the center of the search window is positioned at the nominal line propagation time after the first TW detection at the opposite terminal, and the peak value found within the search window is assumed to be the exit time of the TWs that leave the line. In the TW87, the samples at which the exit TWs are detected at the local e remote terminals are called NL_{EXIT} and NR_{EXIT}, respectively;

3) As soon as the exit TWs are detected, for the sake of security, the amplitude values I_{OP} and I_{RT} are estimated from the current signals i_{OP} and i_{RT} described in (1) and (2). To do so, M samples around NL_{FIRST}, NR_{FIRST}, NL_{EXIT} and NR_{EXIT} are used to estimate I_{OP} and I_{RT}, being $M=T_{DS}/2$ [4]. As a result, the following formulas are used:

$$I_{OP} = C \cdot \sum_{k=-M}^{k=M} \left[i_{TWL}(NL_{FIRST} - k) + i_{TWR}(NR_{FIRST} - k) \right], \quad (5)$$

$$I_{RT} = \max[\, I_{RTL}, I_{RTR}\,], \quad (6)$$

being:

$$I_{RTL} = C \cdot \left| \sum_{k=-M}^{k=M} \left[i_{TWL}(NL_{FIRST} - k) - i_{TWR}(NR_{EXIT} - k) \right] \right|, \quad (7)$$

$$I_{RTR} = C \cdot \left| \sum_{k=-M}^{k=M} \left[i_{TWR}(NR_{FIRST} - k) - i_{TWL}(NL_{EXIT} - k) \right] \right|, \quad (8)$$

where C is a scaling factor adjusted to maintain an unity gain of the estimated amplitudes [4].

4) To improve the TW87 security, additional conditions are evaluated before the tripping decision [4], [7]. The TW87 also analyzes the amplitudes I_L and I_R of the first incident TWs at local and remote terminals, respectively. According to [4], [7], I_L and I_R are estimated using:

$$I_L = C \cdot \sum_{k=-M}^{k=M} i_{TWL}(NL_{FIRST} - k), \quad (9)$$

$$I_R = C \cdot \sum_{k=-M}^{k=M} i_{TWR}(NR_{FIRST} - k) \cdot \quad (10)$$

From I_L and I_R, the TW87 identifies TWs with energy enough to provide a reliable protection operation [7]. Besides, the TW87 also estimates the fault distance m_{87} (in pu) by using the classical TW-based two-terminal fault location formula:

$$m_{87} = 0.5\left(1 + \frac{NL_{FIRST} - NR_{FIRST}}{T_L}\right), \quad (11)$$

where T_L is τ given in number of samples [4].

While external faults result in $m_{87} \approx 0$ or 1 pu, for internal faults, $0 < m_{87} < 1$. Thus, by analyzing m_{87}, the TW87 reliably distinguish internal faults from external events or switching maneuvers at the line terminals.

The TW87 tripping logic is depicted in Figure 2. Modal quantities referenced to each line phase are used to compute I_{OP}, I_{RT}, I_L, I_R and m_{87}, guaranteeing the TW87 operation for all fault types [7]. Also, other additional operation conditions are also taken into account, among which the polarizing voltage (VPOL) supervision and overcurrent supervision (OC87) deserve attention.

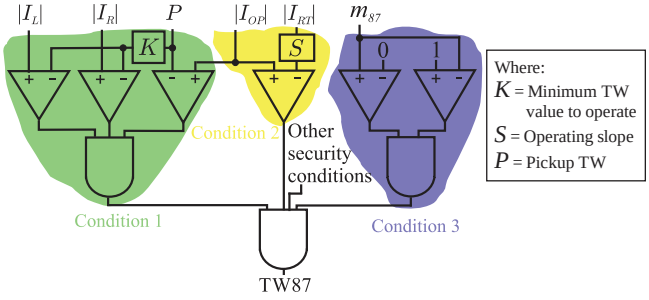

Figure 2: Simplified TW87 tripping logic.

3 Applying the TW87 on HTLs

3.1 Problems Due to the UCL Section Length

When the TW87 is applied on HTLs, some challenges arise. Figure 3 illustrates the Lattice diagrams for internal and external faults on a two-segment transmission line composed by an OTL section with length equal to L_A, and by an UCL section, with length L_S. In the presented example, consider that fault-induced TWs propagate faster in the OTL section.

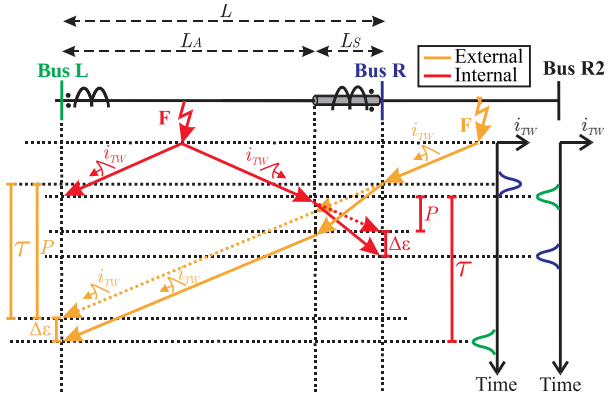

Figure 3: Propagation of fault-induced TWs on HTLs.

Comparing Figures 1 and 3, and supposing that the illustrated HTL was approximated to an uniform OTL, it is noticed that deviations show up in the estimated arrival times of the first incident TWs due to the different propagation velocities in the OTL and UCL sections [7]. In fact, as shown in the figure, the TWs reduce their propagation velocity when they pass from the OTL to the UCL section, resulting in a delayed TW detection. On the other hand, an early detection in relation to the expected one would occur in cases of faults within the UCL section, since the fault-induced TWs accelerate when they pass from the UCL to the OTL.

From Figure 3, it can be seen that the estimated period P is greater than its expected value in internal fault cases. However, since underground cable sections in typical HTLs are usually short, $P < \tau$ is still verified, so that a correct TW87 operation for internal faults is guaranteed. On the other hand, being the measured P value greater than the expected one, the detection of exit TWs may be compromised, since these exit wavefronts can take place outside the search window positioned one line propagation time after the first TW detection at the opposite terminal. As a result, the I_{RT} value varies depending on the UCL length L_S, what may jeopardizes the TW87 security in external fault cases.

Figure 4 illustrates an external fault case downstream from the remote line terminal. The figure shows the detection of exit TWs, when the length L_S of the underground cable section varies. Also, Figure 4 depicts the search windows used to identify the exit TWs that leave the protected line, as well as the calculation window with $2M$ samples applied from (5) to (10) to compute I_{OP}, I_{RT}, I_L and I_R. It should be noted that the calculation window contains M samples before and after the peak value detected within the search window, thereby both windows are not necessarily aligned.

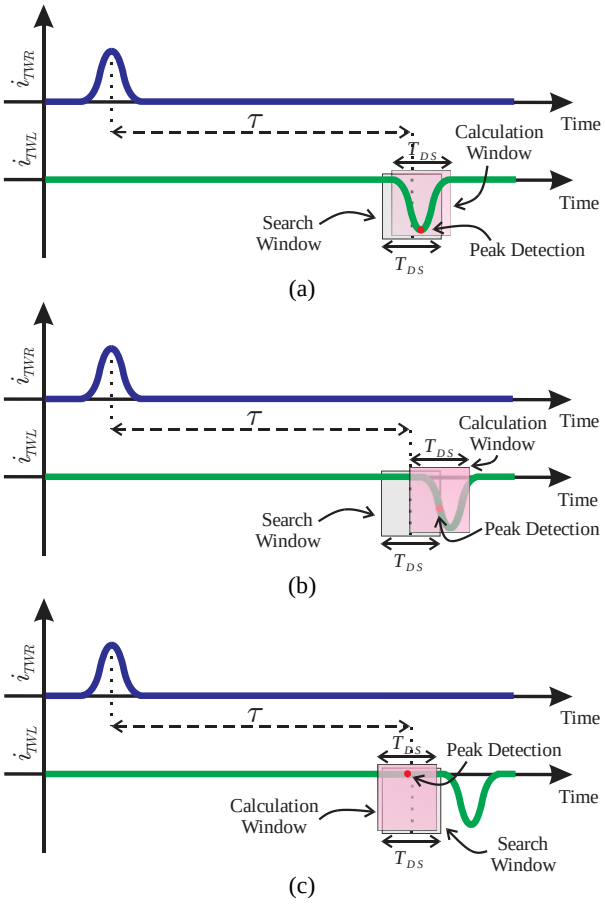

Figure 4: Exit TWs detection and amplitude estimation in HTLs: (a) Underground cable section with negligible length (b) Underground cable section 1.5 km long (c) Long underground cable section.

In Figure 4, the peak detection consists of the identification of the maximum value found within the search window. Hence, even if small time displacements of the exit TWs occur due to the different HTL propagation velocities, the calculation window accommodates most of the errors, since it encompasses the actual peak value related to the exit TW. Thereby, by using (6), an acceptable estimation of I_{RT} is obtained, and a reliable and secure TW87 operation is guaranteed. However, if the time displacement of the exit TWs increases, the peak detection may occur far from the actual peak position, so that the calculation window do not encompasses the exit TW peak value. As a consequence, the errors due to the different propagation velocities on the HTL are not accommodated by the calculation window, and the exit TW is lost, resulting in a reduced value of I_{RT}. Therefore, depending on the length of the UCL section of the monitored HTL, in external fault cases, I_{RT} can present values smaller than I_{OP}, what would compromise the TW87 security.

To solve the abovementioned problems, the TW87 developers suggest the use of an equivalent line propagation time, including the effects of the different parameters of both OTL and UCL sections. Otherwise, if the HTL is approximated to an uniform OHL, restrictions are made regarding the UCL length L_S, which must be shorter than 2 km, as reported in [7].

3.2 Problems Due to the UCL Total Impedance

The TW87 function applies additional security layers to guarantee reliable operations in practical cases of faults in parallel lines, lightning strokes, among other scenarios [4]. Among these security conditions, the overcurrent supervision, called here OC87, and the polarizing voltage (VPOL) supervision deserve attention [7].

The VPOL supervision compares the polarities of I_{OP} and the polarizing voltage, which consists of an estimate of the pre-fault voltage at the fault point obtained from the analysis of the estimated fault location m_{87} and the instantaneous voltage values at both local and remote terminals taken immediately before the detection of the first TWs. Therefore, the TW87 function restrains if both signals have different polarities. On the other hand, to verify if the detected event is a fault and not other low-energy event, the OC87 compares over the time the integrated incremental replica currents with an integrated overcurrent pickup setting plus a security margin (SM) [7]. Therefore, as soon as the integrated incremental replica current presents values greater than the pickup+SM, a fault is confirmed and the TW87 is enabled to operate by the conditions shown in Figure 2.

When applying the TW87 on HTLs, the inclusion of an UCL section in series with the OTL section changes the voltage profile and fault currents along the monitored line in comparison to the case of an uniform OTL. Even approximating the two-segment to an uniform OTL by disregarding the UCL section, differences in voltage profile and fault currents are observed. In this context, it is known that the errors illustrated in Figure 3 lead m_{87} to also present errors, resulting in inaccuracies in the computed polarizing voltage VPOL. However, from preliminary results, for fault cases in a single-circuit transmission line, such a condition tends to be satisfied for most practical scenarios. Thus, as in this paper only a single-circuit HTL is evaluated, only the OC87 supervision will be analyzed in the next sections.

Here, the OC87 is set following the instructions reported in [9]. By doing so, the OC87 may be adjusted to be as sensitive as desired. However, the inclusion of an UCL in the HTL circuit results in a different value of the total impedance of the monitored system, so that the fault current contributions are reduced. As a result, settings computed for an uniform OTL may do not suit for a HTL, in such a way that a restriction regarding the percentage between the total impedance of the UCL (Z_{cable}) and the total impedance of the monitored HTL (Z_{total}) must be taken into account to guarantee the TW87 sensitivity in internal fault cases. In [7], the TW87 developers state that the positive and zero sequence impedance relation (Z_{cable}/Z_{total}).100% must be smaller than 5%. By meeting such a requirement, the TW87 operation is guaranteed even if the HTL is approximated to an uniform OTL. Thus, from the considerations shown in this section, it is concluded that the effects of the UCL section length are cause of concern during external faults, whereas the evaluation of the UCL total impedance is related to the OC87 sensitivity in internal fault cases. These conclusions underlie the computational tests presented next.

4 Test Power System and Simulation

The 230 kV/60 Hz power system shown in Figure 5 was modeled in the ATP to evaluate the TW87 performance when applied on HTLs. The electrical parameters of the modeled system were taken from the Brazilian power grid, which are shown in Tables 1 and 2. Besides the HTL, two adjacent OTLs 100 km long were taken into account to evaluate external fault cases. Thévenin equivalent circuits were used to represent the power systems connected to the adjacent lines. Also, an ATP time step equal to 0.1 μs was used, and a 1 MHz sampling frequency was simulated.

To evaluate the TW87 performance itself, CTs and the communication channel were intentionally modeled as ideal. However, for the simulated line, a communication latency of about 2 ms would be realistic for optical fiber-based links [8], including relay transmit, receive and processing delays.

Due to space limitations, to evaluate problems related to the UCL length, only external AG solid faults with inception angles equal to θ=90º at the middle of the adjacent lines Adj1 and Adj2 were analyzed. Here, two different scenarios were taken into account: Scenario 1) The HTL is approximated by an uniform OTL. In this case, L_S varies from 0.1 km to 6 km with steps of 0.1 km, so that L_A=L-L_S; Scenario 2) The HTL is approximated by an uniform OTL. In this case, L_A is fixed at 200 km, and L_S varies from 0.1 km to 4 km with steps of 0.1, so that L=L_A+L_S (L varies when L_S varies).

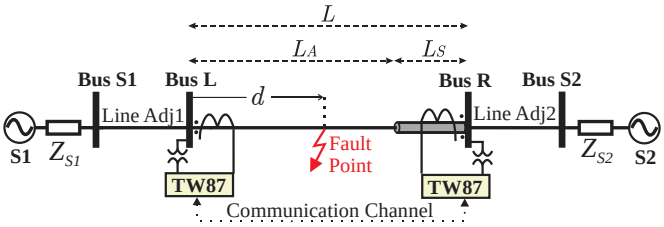

Figure 5: Test System Power.

Transmission Line	*Sequence*	*R (Ω/km)*	*X (Ω/km)*	*ωC (μS/km)*
Overhead	Zero	0.38638	1.42623	2.3057
	Positive	0.10113	0.52381	3.2509
Underground	Zero	0.23000	1.15000	8.0135
	Positive	0.23000	0.23000	40.2153
Adjacent	Zero	0.38638	1.42623	2.3057
	Positive	0.10113	0.52381	3.2509

Table 1: Electrical parameters of transmission lines.

Source	*Voltage (p.u.)*	*Zero Sequence (Ω)*	*Positive Sequence (Ω)*
S1	1.00∟0º	15.4552+j57.0492	4.0452+j20.9524
S2	0.95∟-25º	15.4552+j57.0492	4.0452+j20.9524

Table 2: Thévenin equivalent parameters.

Figure 6 shows the obtained $|I_{OP}|$ and SLP·I_{RT} for the Scenario I when the HTL is approximated by an uniform OTL with length L_A. It is observed that in cases of faults within the adjacent line Adj1 (at the opposite side of the UCL section), $|I_{OP}|$<SLP·I_{RT} is obtained, as expected for external fault cases. However, for faults within the adjacent line Adj2 (at the same

side of the UCL section), $|I_{OP}|$>SLP·I_{RT} is verified for L_S>1 km when SLP=0.5, and for L_S>4.2 km when SLP=0.6, leading the TW87 to misoperate. Similarly, from Figure 7, which shows $|I_{OP}|$ and SLP·I_{RT} for the Scenario II when the HTL is approximated by an uniform OTL 200 km long, in cases of faults within the adjacent line Adj1, $|I_{OP}|$<SLP·I_{RT} is obtained, so that the TW87 correctly restrains as expected. Nevertheless, for faults within the adjacent line Adj2, again, the TW87 misoperates, because $|I_{OP}|$>SLP·I_{RT} for L_S>1 km when SLP=0.5, and for L_S>2.5 km when SLP=0.6. Therefore, assuming SLP=0.6, Figures 6 and 7 justify the restrictions suggested by the TW87 developers, which state that the UCL section should not have lengths greater than 2 km [7].

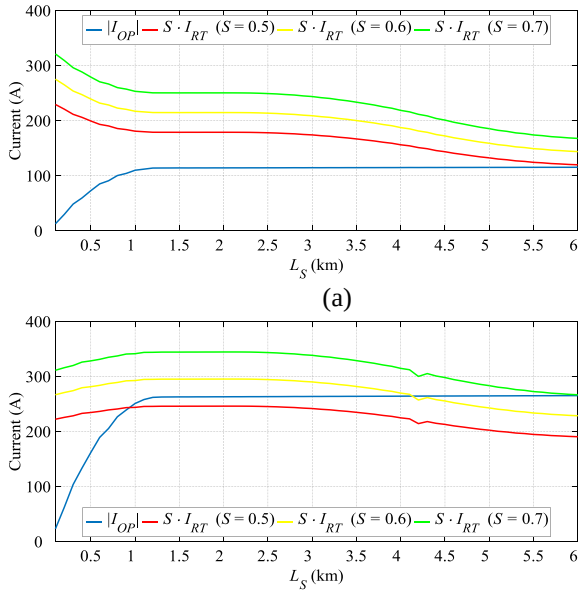

(a)

(b)

Figure 6: Scenario I for faults on lines: (a) Adj1; (b) Adj2.

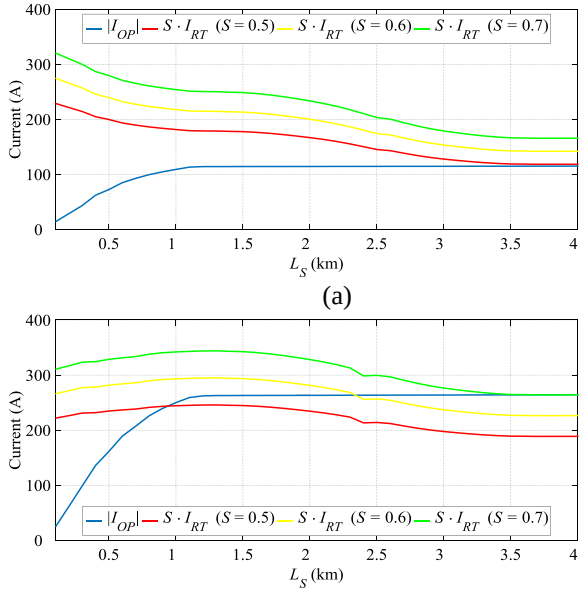

(a)

(b)

Figure 7: Scenario II for faults on lines: (a) Adj1; (b) Adj2.

Based on Figures 6 and 7, one concludes the critical values of L_S in Scenarios I and II for SLP=0.6 were of about 4 km and 2.5 km, respectively. Hence, to evaluate the L_S variation and the percentage relation (Z_{cable}/Z_{total}).100% on the OC87 supervision, AG fault currents I_F were computed for several combinations of (Z_{cable}/Z_{total}).100% and fault distances d. The obtained results are shown in Figures 8 and 9, where the OC87 threshold TP50G is represented by the sum of the overcurrent pickup plus a security margin SM. By doing so, cases in which the OC87 supervision loses its sensitivity in internal fault cases due to the presence of the UCL section in the monitored HTL are identified.

From Figures 8 and 9, by using SM as a percentage of 0.5% and 1% of the OC87 pickup setting (resulting in the threshold TP50G), it is noted that the OC87 supervision blocks the TW87 operation in some cases, depending on the combination of SM and (Z_{cable}/Z_{total}).100%. As shown in Figure 8, in Scenario I, the OC87 blocks the TW87 for (Z_{cable}/Z_{total}).100%≈5.4% and 8%, when SM=0.5% and 1% of the OC87 pickup, respectively. On the other hand, as shown in Figure 9, in Scenario II, the OC87 supervision blocks the TW87 for (Z_{cable}/Z_{total}).100%≈4.3% and 8%, when SM=0.5% and 1% of the OC87 pickup, respectively.

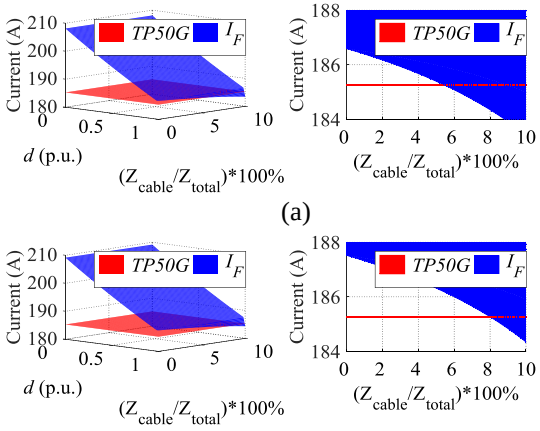

(a)

(b)

Figure 8: OC87 evaluation in Scenario I for SM equal to: (a) 0.5% of TP50G; (b) 1% of TP50G.

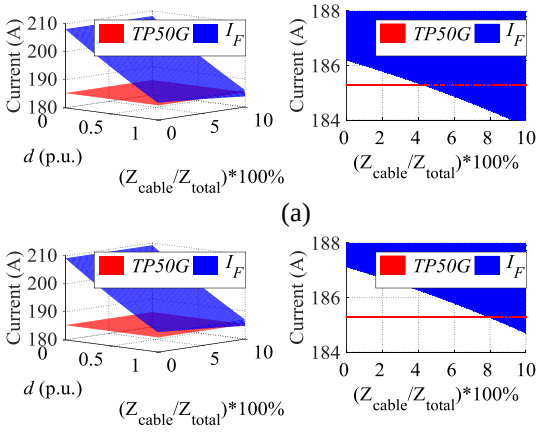

(a)

(b)

Figure 9: OC87 evaluation in Scenario II for SM equal to: (a) 0.5% of TP50G; (b) 1% of TP50G.

Based on the obtained results for the evaluated system, it is concluded that (Z_{cable}/Z_{total}).100% greater than ≈ 4.3% must be avoided when applying the TW87 on HTLs. By considering this restriction, the OC87 operation for faults at any point of the HTL is guaranteed. In fact, such a critical value is very close to the restriction of the (Z_{cable}/Z_{total}).100% value reported by the TW87 developers in [7], where a maximum (Z_{cable}/Z_{total}).100% value equal to 5% is indicated. Thereby, it is concluded that by using the special requirements reported by the TW87 developers, the TW87 can properly protect HTLs, without loss of security and sensitivity.

Finally, it should be pointed out that, if Z_{cable} is taken into account during the OC87 setting, sensitive TP50G values may be obtained, guaranteeing its operation for faults at any point of the HTL. Besides, if the equivalent line propagation time of the HTL is taken into account, I_{RT} deviations due to the exit TW displacements in time are eliminated. However, since the TWs transmitted from the OTL to the UCL are amplified, and those transmitted from the UCL to the OTL are attenuated, I_{RT} amplitude variations may show up, so that an appropriate SLP value should be chosen. Figure 10 illustrates the results obtained for the Scenario I when the equivalent line propagation time is taken into account. For faults within the adjacent line Adj1, the TW87 function operated as expected for all evaluated L_S values. On the other hand, for faults within the adjacent line Adj2, although in the case of SLP=0.5 the TW87 misoperates for L_S>1 km, it is observed that the problems shown in Figure 6 are overcome when SLP=0.6 and 0.7 are used, leading the TW87 to operate as expected for all evaluated L_S values. Therefore, it is concluded that by using appropriate TW87 settings, the TW-based differential protection scheme may protect HTLs, without restrictions related to the UCL length L_S.

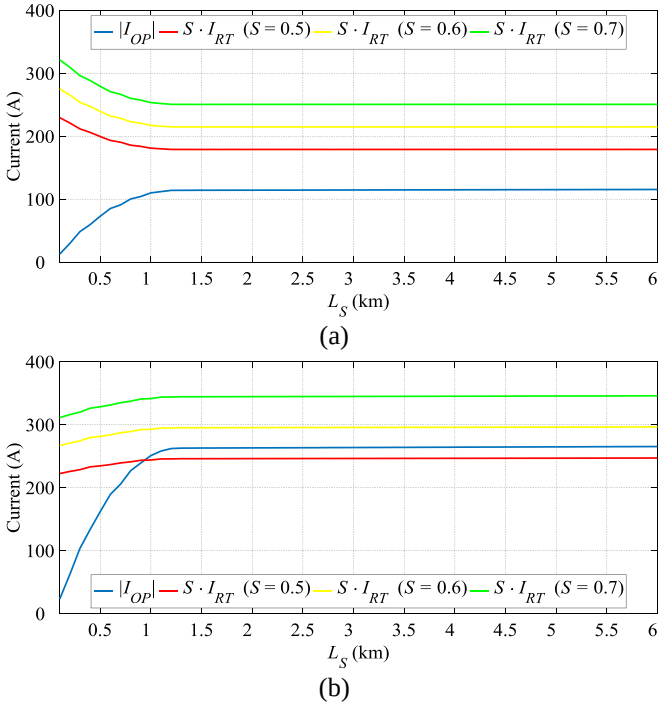

Figure 10: Scenario I, considering an equivalent line propagation time for faults on lines: (a) Adj1; (b) Adj2.

5 Conclusions

In this paper, issues related to the application of the TW-based differential protection function (TW87) on hybrid lines were addressed. The main challenging scenarios were presented and evaluated, highlighting some special requirements related to the underground cable section length and impedance that must be taken into account when the hybrid line is approximated to an uniform overhead line. Finally, it was attested that simple adaptations on the TW87 settings may guarantee reliable and secure protection operations, irrespective of the underground cable section length and impedance.

Acknowledgements

The authors would like to thank the Federal District Research Support Foundation (FAP-DF) and the Coordination for the Improvement of Higher Education Personnel (CAPES) for the financial support.

References

[1] P. M. Anderson, *Power System Protection*. Piscataway, New Jersey, EUA: John Wiley & Sons Inc., (1999).

[2] E. O. Schweitzer, B. Kasztenny, A. Guzmán, V. Skendzic, and M. V Mynam, "Speed of line protection - can we break free of phasor limitations?," in *68th Annual Conference for Protective Relay Engineers*, (2015).

[3] E. O. Schweitzer, B. Kasztenny, M. V Mynam, A. Guzmán, N. Fischer, and V. Skendzic, "Defining and Measuring the Performance of Line Protective Relays under the title " Defining and Measuring the Performance of Line Protection Relays " 1 Defining and Measuring the Performance of Line Protective Relays," (2016).

[4] E. O. Schweitzer, B. Kasztenny, and M. V Mynam, "Performance of Time-Domain Line Protection Elements on Real-World Faults," in *42nd Annual Western Protective Relay Conference*, (2015).

[5] D. A. Tziouvaras and J. Needs, "Protection of mixed overhead and underground cable lines," in *12th IET International Conference on Developments in Power System Protection (DPSP 2014)*, (2014).

[6] C. Jensen, *Online Location of Faults on AC Cables in Underground Transmission Systems*, 1st ed. Springer International Publishing, (2014).

[7] SEL T400L - "Ultra-High-Speed Transmission Line Relay Traveling-Wave Fault Locator High-Resolution Event Recorder." *Instruction Manual*, (2016).

[8] E. O. Schweitzer *et al.*, "Locating Faults by the Traveling Waves They Launch," (2014).

[9] B. Kasztenny, A. Guzmán, N. Fischer, M. V Mynam, and D. Taylor, "Practical Setting Considerations for Protective Relays That Use Incremental Quantities and Traveling Waves.", (2016).